Bending contorted hexabenzocoronene into a bowl†

Adam C. Whalley,[a] Kyle N. Plunkett,[b] Alon A. Gorodetsky,[a] Christine L. Schenck,[a] Chien-Yang Chiu,[a] Michael L. Steigerwald*[a] and Colin Nuckolls*[a]

Received 6th September 2010, Accepted 24th September 2010
DOI: 10.1039/c0sc00470g

This article describes the synthesis of a new type of bowl-shaped polycyclic aromatic hydrocarbon. These bowls are formed by joining the proximal carbons of contorted hexabenzocoronenes. These methods begin to tap a wealth of structural diversity available from these core structures. The bowl-shaped hydrocarbons more easily accept electrons than their contorted hexabenzocoronene precursors and associate strongly with C_{70}.

This article describes the preparation and photophysical properties of a new type of bowl-shaped polycyclic aromatic hydrocarbon (PAH) formed by joining the proximal carbons of contorted hexabenzocoronenes. Contorted hexabenzocoronenes[1] are a class of compounds that have six 4-carbon annulations circumferential to coronene (**1**). This structure is highly non-planar as a result of the steric congestion around its periphery. Previously, we found these molecules dehydrogenate upon heating on a ruthenium surface to form highly curved structures.[2] The main dehydrogenated product was assigned a structure in which six 5-membered rings had formed between its proximal carbons. These compounds are interesting because they represent a new class of bowl-shaped PAHs.[3–7] Unfortunately, the resulting bowl-shaped molecules are so tightly bound to the metal surface that they could not be freed from the surface for further study. Here we develop the solution-based chemistry to synthesize and study two members of this class of PAHs with two and four of their five-membered rings formed (**2** and **3**, respectively). We find that the resulting compounds are highly non-planar, are bowl-shaped, and complex strongly with C_{70}.

Fig. 1 shows the structural diversity resulting from the closure of the five-membered rings around the coronene core: twelve structural siblings that differ in the quantity and position of the five-membered rings. In addition, several of the compounds can exist in multiple conformations. The molecular shape of each analog varies significantly with subsequent five-membered ring incorporation. We focused this study on **2** and **3** because they were synthetically accessible and DFT calculations predicted the emblematic bowl architecture. Furthermore, our earlier computational studies[8] showed that the compounds with four five-membered rings closed are the most energetically disfavored of the compounds in Fig. 1 due to their high degree of curvature.

The DFT-optimized structures of **2** and **3** (B3LYP functional with the 631G** basis set) are shown in Fig. 2 and 3, respectively. Similar to previously crystallized contorted HBCs,[1] the three "free" annulated benzo-substituents in **2** (rings b, c and b′ in Fig. 2A) are contorted and follow a down-up-down arrangement. The conformational isomer where the arrangement of b, c, and b′ is up-down-up is ~7.5 kcal mol^{-1} higher in energy than the structure in Fig. 2. The bowl of **2** is composed of three annulated benzene rings connected through two five-membered rings and is concave above the two adjacent benzene rings. The splay angle (defined in Fig. 2A) between the a/b rings (38°) and the b/c rings (39°) provides a measure for the degree of strain inherent to these subunits. For comparison, the exterior ring splay for **1** is 42° while that for 4-helicene is 31°.[9] We conclude that the newly formed five-membered rings pull the benzo-substituents back to alleviate some of the steric congestion around the periphery. These rings are further pulled back in **3** where the splay angle between the two rings that are not joined by five-membered rings is a mere ~3°. The locus of the majority of strain in **3** is in its bowl-shaped portions and not in the 4-helicene subunits.

The bowl in **2** has a high degree of curvature and the π-orbital axis vector (POAV) pyramidalization angles,[10,11] defined as $\theta_{\sigma\pi} - 90°$, were calculated to be 8.5°, 8.3°, and 4.6° for the most distorted carbon atoms in the central area of the bowl in **2** (shown in Fig. 2A). These values are slightly greater than those of corannulene (8.2°)[12] but less than C_{60} (11.6°).[11] Compound **3** contains two cupped regions that slightly increased the strain on the most interior carbons with the POAV angles calculated to be 8.4°, 7.3°, and 5.8° (shown in Fig. 3A).

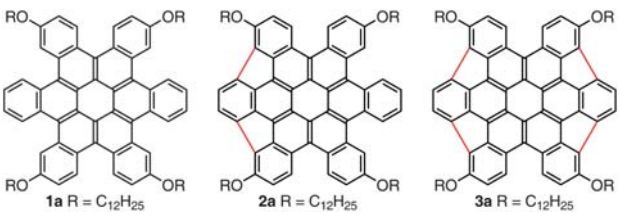

Our syntheses of **2** and **3** relied on n-dodecyloxy hydrocarbon chains (**2a** and **3a**) to ensure solubility throughout. These compounds were derived from HBC precursors that would allow us to employ the solution-based, palladium-catalyzed chemistry, which was pioneered by Scott[4] and Shevlin,[3,13] to form the strained, five-membered rings. These heavily substituted HBC derivatives (**5a,b**) were synthesized from the corresponding halogenated pentacenequinone cores (**4a,b**) as shown in Scheme 1.[14,15] For the final ring closure, converting **5a** to **2a**, we exposed the compound to microwave-assisted Heck conditions using

[a]*Department of Chemistry, Columbia University, New York, NY, USA. E-mail: cn37@columbia.edu; mls2064@columbia.edu; Fax: +212 932 1289; Tel: +212 854 6289*
[b]*Department of Chemistry, Southern Illinois University, Carbondale, IL, USA*
† Electronic supplementary information (ESI) available: Experimental and computational details. See DOI: 10.1039/c0sc00470g

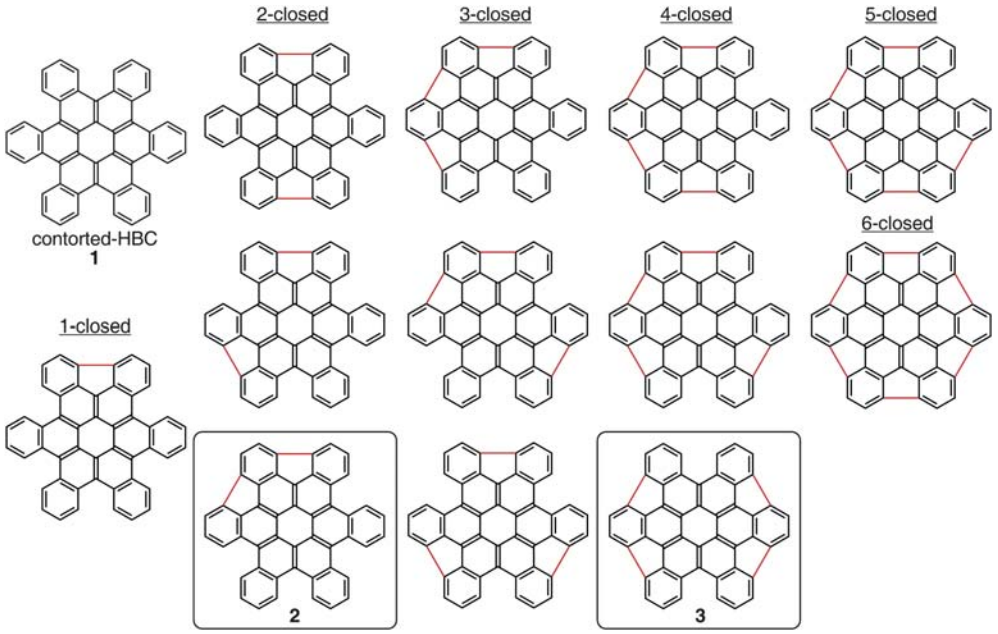

Fig. 1 Illustration of the structural diversity available *via* closure of the 5-membered rings around the exterior of hexabenzocoronene (**1**). Derivatives of the structures highlighted with boxes (**2**, **3**) were synthesized in this study.

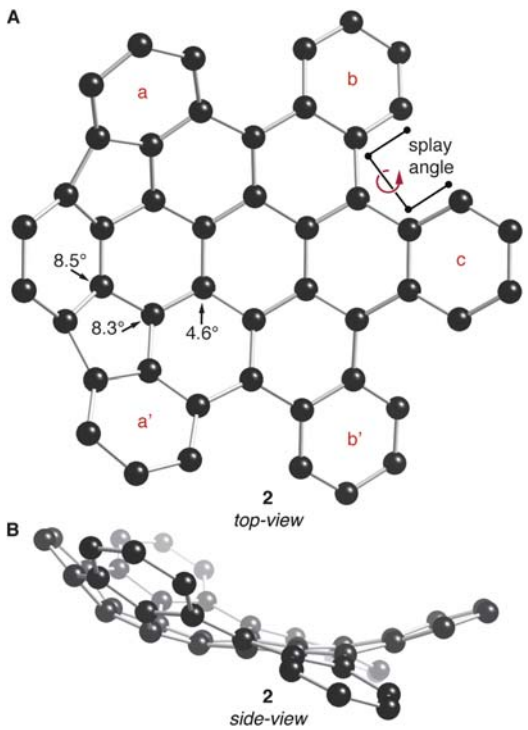

Fig. 2 (A) Top- and (B) side-view of the DFT calculated structure of **2**. POAV angles at their corresponding carbon atoms. Carbons are shown with black spheres. Hydrogen atoms have been removed for clarity.

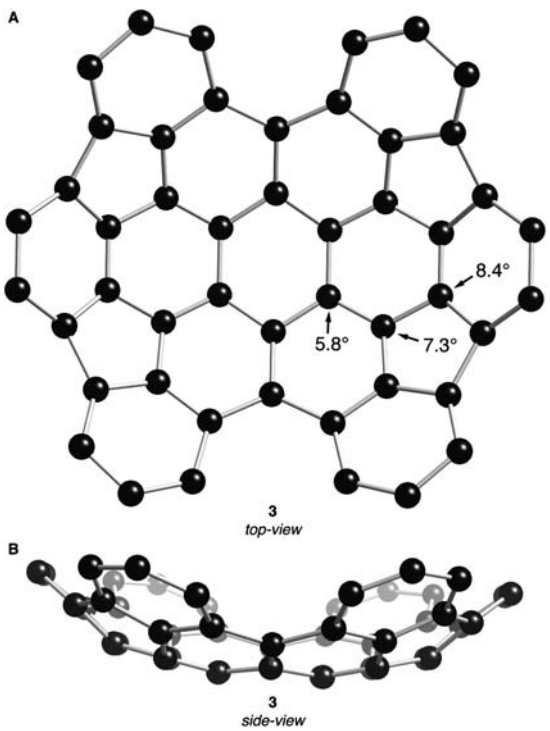

Fig. 3 (A) Top- and (B) side-view DFT calculated structure of **3**. POAV angles at their corresponding carbon atoms. Carbons are shown with black spheres. Hydrogen atoms have been removed for clarity.

$[Pd(PCy_3)_2Cl_2]$ as the catalyst and DBU as the base. The double ring-closure proceeded smoothly and **2a** was isolated as a red solid in 82% yield. In a similar reaction with **5b**, **3a** formed in good yield (as indicated by ^{1}H-NMR), but it was difficult to separate **3a** from the derivative in which only three of the 5-membered rings formed, the fourth position being simply dehalogenated.[16] Successive chromatographic separations gave pure **3a** as a red solid in 16% yield.

The thermal inversion barriers for the bowls are quite high. By observing the coalescence of diastereotopic methylene hydrogens with variable temperature NMR, we determined an inversion barrier of 18.5 kcal mol^{-1} in **2a** (complete coalescence occurs at

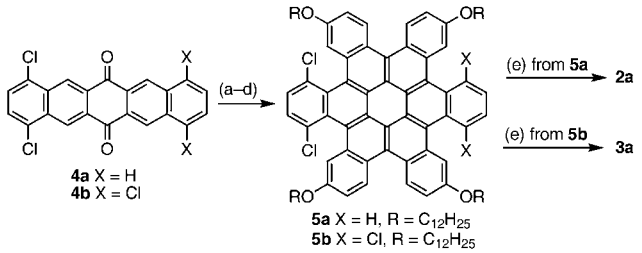

Scheme 1 Synthesis of **2a** and **3a**. Key: (a) CBr_4, PPh_3, toluene, 80 °C, 16 h. (b) $[Pd(PPh_3)_4]$, 2-(4-(dodecyloxy)phenyl)-4,4,5,5-tetramethyl-1,3,2-dioxaborolane, THF, 2 M K_2CO_3 (aq), 100 °C, 16 h. (c) hν, I_2, benzene, propylene oxide, 3 h, rt. (d) $FeCl_3$, CH_3NO_2, CH_2Cl_2, 3 h, rt. (e) $[Pd(PCy_3)_2Cl_2]$, DBU, DMA, μwave, 150 °C, 3 h.

95 °C). As a point of comparison the tetra-dodecyloxy HBC (**1a**) inversion barrier is 16.7 kcal mol^{-1} (65 °C).[17] **3a** also showed diastereotopic methylene hydrogens; however, we observed no coalescence even upon heating to 180 °C. This suggests that **3a** is conformationally locked and unable to invert on the NMR timescale at 180 °C.[18]

HBCs are generally yellow whereas the bowls, **2a** and **3a**, are red. This shift in color suggests that the induced curvature substantially changes the electronic structure. The UV-vis spectra of compounds **1a–3a** can be seen in Fig. 4. Compound **1a** has a typical absorbance with a λ_{max} at 380 nm and only weak absorbance above 425 nm.[1,19] Compound **2a** shows a very slight blue-shift of the λ_{max} to 377 nm but the longer-wavelength transition gains significant intensity. Compound **3a** shows an overall red-shift of both the λ_{max} to 392 nm as well as a broad absorbance above 425 nm. The sequential closures of the five-membered rings do not have a monotonic effect on the position of the lowest-energy optical absorptions of **1a–3a** as **2a**'s absorption extends to the longest wavelength of the three.

To understand this trend in the UV-vis absorbance, we undertook electronic structure calculations. Time-dependent DFT calculations (modeling the tetramethoxy analogs) showed that in all three molecules the lowest-energy, spin-allowed excitations are primarily from the HOMO to the LUMO. In each case, the HOMO is one of the radialene π set, but while the LUMO of **1** is one of the radialene π* orbitals, the LUMO in **2** and **3** are closely associated with the new five-membered rings.

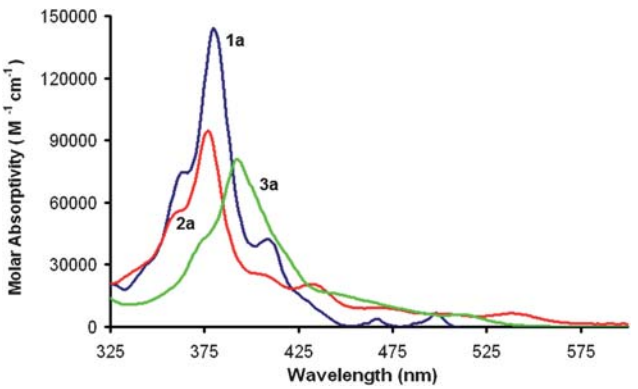

Fig. 4 UV-vis spectra of **1a** (blue), **2a** (red), and **3a** (green) in CH_2Cl_2. Concentration = 3.00×10^{-6} M, $l = 1$ cm.

This suggests the development of cyclopentadienide character in the new rings, a suggestion that is substantiated by the decrease in LUMO energies (−1.6 eV, −2.0 eV, and −2.1 eV in **1**, **2**, and **3**, respectively). This trend alone would predict that **3** would absorb to the red of **2**, however the trend in HOMO energies (−4.8 eV, −4.8 eV, and −5.0 eV) belies this. The HOMO energy in **3** is lowered because the two radialene $R_2C{=}CR_2$ arrays that host the HOMO are closer to planar than are the corresponding sites in **1** and **2** (See Supporting Information). Thus while closing the five-membered rings does monotonically lower the energy of the LUMO, the effect on the HOMO is not so uniform.

Cyclic voltammetry (see Table 1) supports the conclusions for the calculated energies of **1a–3a**. The oxidation potentials of **1a** and **2a** are roughly the same, but that of **3a** is significantly higher. This is the same trend that we observe with the HOMO energies from DFT. The reduction potentials similarly map the LUMO landscape: the highest energy reduction is roughly equivalent throughout the three molecules and represents reduction of the core. Additionally, for each aromatic five-membered ring there is an additional low-energy reduction: **2a** shows two reductions (core plus one cyclopentadienide), and **3a** shows three reductions (core plus two cyclopentadienides). These results further exemplify the ability of bowl-like structures to stabilize negative charges.[20] This feature hints that these materials may be useful as n-type organic semiconductors in thin film devices.

The fluorescence emission spectra of compounds **1a–3a** show a dramatic reduction in light emission, as well as a general red shift, when the number of five-membered rings increases (Fig. 5A). While **1a** is highly fluorescent with a quantum yield of 0.14 (CH_2Cl_2), the quantum yields of **2a** and **3a** were determined to be 0.034 and 0.0085 (CH_2Cl_2), respectively. The apparent fluorescence dampening is reminiscent of fullerenes, which have quantum yields on the order of 1×10^{-4}, as well as other small molecules containing five-membered rings that display no detectable fluorescence.[20]

Recently, we showed that HBC co-crystallized with C_{60} in a 1 : 2 or 1 : 1 stoichiometry in the solid state.[21] The favorable interactions between the π-face of the contorted HBC and the fullerene drive this co-crystallization. **2a** and **3a** have a more defined bowl-like structure that should allow them to interact with fullerenes more intimately. We initially chose C_{70} as a guest molecule as it has an oval shape that is more shape complementary to **3a**. Our test for binding was to monitor the fluorescence quenching when equimolar amounts of C_{70} were added to **1a–3a**. No measurable decrease in emission intensity was found for C_{70} and **1a** at equimolar concentrations in CH_2Cl_2 (Supporting Information), suggesting that the association between **1** and C_{70} is minimal in solution. **2a** emission is quenched by about

Table 1 Cyclic voltammetry redox potentials[a]

	E^1_{ox}	E^2_{ox}	E^1_{red}	E^2_{red}	E^3_{red}
1a	1.08	1.32	–1.77[b]	—	—
2a	1.12	1.46	–1.38	–1.72	
3a	0.98[b]	1.32[b]	–1.37	–1.53	–1.89[b]

[a] Potentials are measured in volts relative to Ag/Ag^+. 1 mM in CH_2Cl_2 with 0.1 M $(Bu_4N)^+$ $(BF_4)^-$. [b] Quasi-reversible or irreversible peaks.

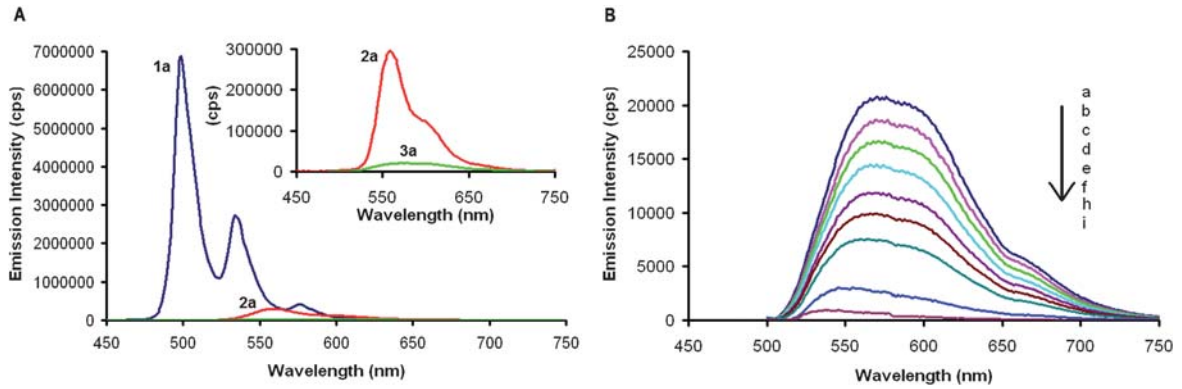

Fig. 5 (A) Fluorescence emission spectra of **1a** (blue), **2a** (red), and **3a** (green) at 1.00×10^{-6} M in CH_2Cl_2. Inset shows the zoomed in region of **2a** and **3a**. (B) Fluorescence emission spectra of **3a** (1.00×10^{-6} M in CH_2Cl_2) excited at 392 nm with: (a) 0, (b) 0.05, (c) 0.10, (d) 0.15, (e) 0.2, (f) 0.25, (g) 0.3, (h) 0.4, and (i) 1.0 molar equivalents of C_{70} added.

50% when it is mixed with equimolar amounts of C_{70} (Supporting Information). **3a** shows completely quenched fluorescence when ~0.5 equivalents of C_{70} is added (Fig. 5B). This demonstrates that the association constants between **2a** and C_{70} as well as **3a** and C_{70} are very high.[22–25] Using a simple Stern–Volmer analysis, an association constant was calculated to be 4.7×10^5 M^{-1} for **2a** and C_{70} and 3.2×10^6 M^{-1} for **3a** and C_{70}.[26]

Conclusions

In conclusion, we have synthesized a new class of bowl-shaped PAHs based on a coronene core. The shallow bowl shape of **3a** shows an enhanced ability to stabilize negative charge and to bind C_{70} very strongly. The unique optical, electronic, and structural properties of these new bowl-shaped PAHs provide opportunities to create new n-type organic materials, phase-compatibilizers between p-type semiconductors and fullerenes in photovoltaic devices, and novel host–guest complexes.

Acknowledgements

This research was funded by the Chemical Sciences, Geosciences and Biosciences Division, Office of Basic Energy Sciences, US D.O.E. (#DE-FG02-01ER15264), by the Center for Re-Defining Photovoltaic Efficiency Through Molecule Scale Control, an Energy Frontier Research Center funded by the U.S. Department of Energy, Office of Science, Office of Basic Energy Sciences under Award Number DESC0001085, and by the FCRP FENA program. C.L.S. wishes to acknowledge support by the NSF GRFP; A.A.G. was supported by the National Science Foundation under Award Number 0936923; and A.C.W. acknowledges the support of the Guthikonda Fellowship in Organic Chemistry.

Notes and references

1 S. Xiao, M. Myers, Q. Miao, S. Sanaur, K. Pang, M. L. Steigerwald and C. Nuckolls, *Angew. Chem., Int. Ed.*, 2005, **44**, 7390–7394.
2 K. T. Rim, M. Siaj, M. Myers, L. Liu, C. Su, M. L. Steigerwald, S. Hybertsen, P. H. McBreen, G. W. Flynn and C. Nuckolls, *Angew. Chem., Int. Ed.*, 2007, **46**, 7891–7895.
3 L. Wang and P. B. Shevlin, *Org. Lett.*, 2000, **2**, 3703–3705.
4 H. A. Reisch, M. S. Bratcher and L. T. Scott, *Org. Lett.*, 2000, **2**, 1427–1430.
5 T. Amaya, T. Nakata and T. Hirao, *J. Am. Chem. Soc.*, 2009, **131**, 10810–10811.
6 B. D. Steinberg, E. A. Jackson, A. S. Filatov, A. Wakamiya, M. A. Petrukhina and L. T. Scott, *J. Am. Chem. Soc.*, 2009, **131**, 10537–10545.
7 H. Sakurai, T. Daiko, H. Sakane, T. Amaya and T. Hirao, *J. Am. Chem. Soc.*, 2005, **127**, 11580–11581.
8 Unpublished data.
9 F. H. Herbstein and G. M. J. Schmidt, *J. Chem. Soc.*, 1954, 3302–3313.
10 R. C. Haddon and L. T. Scott, *Pure Appl. Chem.*, 1986, **58**, 137–142.
11 R. C. Haddon, *J. Am. Chem. Soc.*, 1990, **112**, 3385–3389.
12 D. Bakowies and W. Thiel, *J. Am. Chem. Soc.*, 1991, **113**, 3704–3714.
13 L. Wang and P. B. Shevlin, *Tetrahedron Lett.*, 2000, **41**, 285–288.
14 C. R. Swartz, S. R. Parkin, J. E. Bullock and J. E. Anthony, *Org. Lett.*, 2005, **7**, 3163–3166.
15 K. N. Plunkett, K. Godula, C. Nuckolls, N. Tremblay, A. C. Whalley and S. Xiao, *Org. Lett.*, 2009, **11**, 2225–2228.
16 The 3-closed HBC contaminant was evident *via* NMR, but we were unable to obtain an analytically pure sample.
17 T. J. Seiders, K. K. Baldridge, G. H. Grube and J. S. Siegel, *J. Am. Chem. Soc.*, 2001, **123**, 517–525.
18 Analogs of **1a**, **2a**, and **3a** were synthesized with two alkyl chains in order to simplify analysis of the variable temperature ^{1}H NMR data (see supplemental information).
19 Y. S. Cohen, S. Xiao, M. L. Steigerwald, C. Nuckolls and C. R. Kagan, *Nano Lett.*, 2006, **6**, 2838–2841.
20 H. Dang, M. Levitus and M. A. Garcia-Caribay, *J. Am. Chem. Soc.*, 2002, **124**, 136–143.
21 N. J. Tremblay, A. A. Gorodetsky, M. Cox, T. Schiros, B. Kim, R. Steiner, Z. Bullard, A. Sattler, W.-Y. So, Y. Itoh, M. F. Toney, H. Ogasawara, A. P. Ramirez, I. Kymissis, M. L. Steigerwald and C. Nuckolls, *ChemPhysChem*, 2010, **11**, 799–803.
22 A. Sygula, F. R. Fronczek, R. Sygula, P. W. Rabideau and M. M. Olmstead, *J. Am. Chem. Soc.*, 2007, **129**, 3842–3843.
23 C. Mück-Lichtenfeld, S. Grimme, L. Kobryn and A. Sygula, *Phys. Chem. Chem. Phys.*, 2010, **12**, 7091–7097.
24 P. E. Georghiou, L. N. Dawe, H.-A. Tran, J. Strübe, B. Neumann, H.-G. Stammler and D. Kuck, *J. Org. Chem.*, 2008, **73**, 9040–9047.
25 A. Molina-Ontoria, G. Fernádez, M. Wielopolski, C. Atienza, L. Sánchez, A. Gouloumis, T. Clark, N. Martín and D. M. Guldi, *J. Am. Chem. Soc.*, 2009, **131**, 12218–12229.
26 V. O. Stern and M. Volmer, *Physik. Zeitschr.*, 1919, **20**, 183–188.

